Electronic Supplementary Information

Determination of ion concentration[1]

Determination of NO_3^--N: First, part of electrolyte after nitrate electroreduction process is taken out from the cathode. The electrolyte was diluted to keep the NO_3^--N within the detection range. Then, 1 M HCl (100 μL) and 0.8 wt% (10 μL) sulfamic acid were added into the diluted electrolyte (5 mL), and the mixture is placed for 10 min before using. UV-Vis spectrophotometry was employed to determine the absorbance of the mixture from 200 nm to 300 nm. Based on the equation of $A = A_{220nm} - 2A_{275nm}$, the final absorbance was obtained. The concentration-absorbance curve was calibrated using different concentrations of KNO_3.

Determination of NO_2^--N: The color reagent was prepared by dissolving 0.8 g p-aminobenzenesulfonamide, 0.04g N-(1-Naphthyl) ethylenediamine dihydrochloride and 2 mL phosphoric acid (ρ=1.70 g/mL) in 10 mL deionized water. Specifically, 0.1 mL of color reagent was added into electrolyte which diluted to detection range. After 20 min, the absorbance value at a wavelength of 540 nm can be determined by the UV-Vis spectrophotometry. The absorbance of $NaNO_2$ was determined at different concentrations to obtain the concentration-absorbance curve.

Determination of $NH_3(NH_4^+)$-N: The concentrations of ammonia can be quantified using Nessler's reagent. Thus, 0.1 mL of 0.5 g/L sodium potassium tartrate solution and 0.1 mL of Nessler's reagent mixed into the electrolyte which was diluted to detection range. After standing for 20 minutes, the wavelength of 420 nm was measured using UV-vis spectrophotometry to reveal the absorbance of NH_4^+-N. The concentration-absorbance curve was obtained by determining the different concentrations of standard NH_4Cl solutions.

^{15}N Isotope Labeling Experiments:

Isotope labelling experiments were performed using $K^{15}NO_3$-^{15}N as a nitrogen source to replace $K^{14}NO_3$-^{14}N, for determining the source of ammonia. The pH of the electrolyte was adjusted to a weak acid by adding 4 M H_2SO_4. For preparation of calibration curve, different concentration of $^{15}NH_4^+$-^{15}N solutions (50, 100, 150, 200, 250 mg L^{-1}) and 50 mg L^{-1} maleic acid were added in 0.5 M K_2SO_4. The D_2O was added aforementioned mixture for the NMR detection. On account of $^{15}NH_4^+$-^{15}N concentration and the area ratio were positively correlated, the calibration curve can be obtained by using the peak area ratio between $^{15}NH_4^+$-^{15}N and maleic acid.

Calculation of the conversion rate, yield, selectivity, and Faradaic efficiency

The calculation of all values is provided by the absorbance measured by the UV-Vis spectrophotometer.

The conversation of NO_3^- was calculate using Eq. S1:

$$\mathrm{NO_3^-}\ \text{Conversion}=\Delta C_{NO_3^-}/C_0\times 100\% \qquad \text{(Eq. S1)}$$

The selective of NH_3 was calculate using Eq. S2:

$$\mathrm{NH_3}\ \text{Selectivity}=C_{NH_3}/\Delta C_{NO_3^-}\times 100\% \qquad \text{(Eq. S2)}$$

The selective of NO_2^- was calculate using Eq. S3:

$$\mathrm{NO_2^-}\ \text{Selectivity}=C_{NO_2^-}/\Delta C_{NO_3^-}\times 100\% \qquad \text{(Eq. S3)}$$

The yield of NH_3 was calculate using Eq. S4:

$$\text{Yield}_{\mathrm{NH_3}}=(C_{NH_3}\times V)/(M_{NH_3}\times t\times S) \qquad \text{(Eq. S4)}$$

The Faradaic efficiency was calculate using Eq. S5:

$$\text{Faradaic efficiency}=(8F\times C_{NH_3}\times V)/(M_{NH_3}\times Q)\times 100\% \qquad \text{(Eq. S5)}$$

where C_{NH3} is the concentration of $NH_{3(aq)}$, C_{NO2}^- is the concentration of $NO_2^-{}_{(aq)}$, ΔC_{NO3^-} is the concentration difference of NO_3^- before and after electrolysis, C_0 is the initial concentration of NO_3^-, V is the electrolyte volume, M_{NH3} is the molar mass of NH_3, t is the electrolysis time, S is the area of catalyst, F is the Faradaic constant (96485 C mol^{-1}), Q is the total charge passing the electrode.

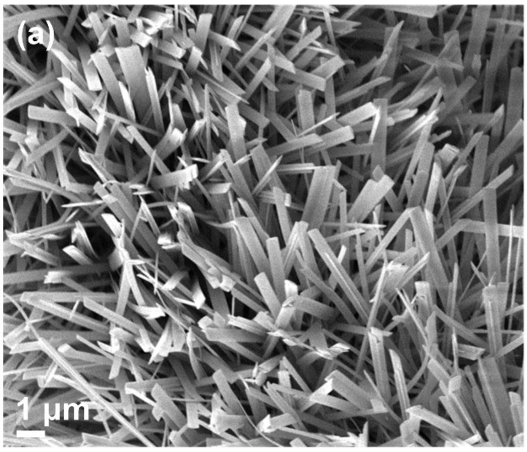

Fig. S1 SEM image of $Cu(OH)_2$/CF.

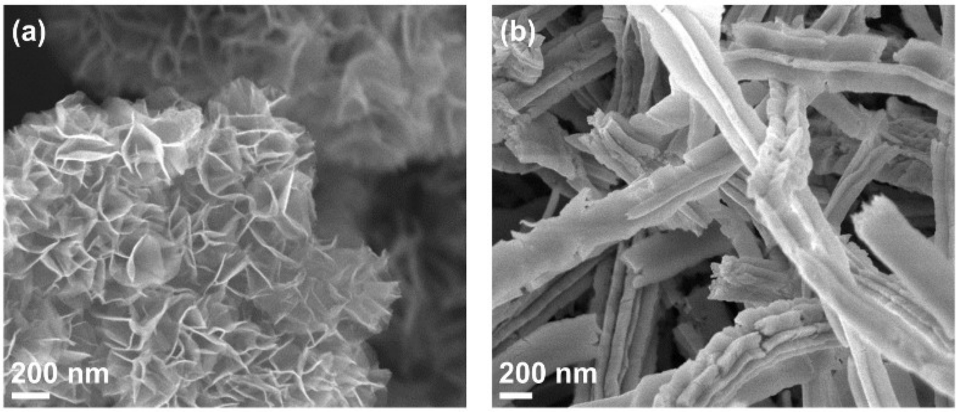

Fig. S2 SEM images of (a) MnO_2 nanosheets and (b) CuO/CF.

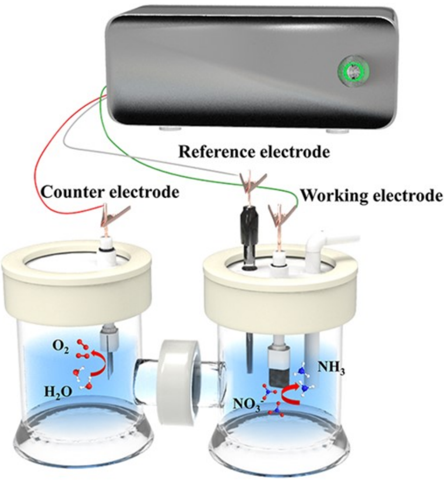

Fig. S3 Schematic illustration showing the electrocatalytic system for nitration reduction to ammonia.

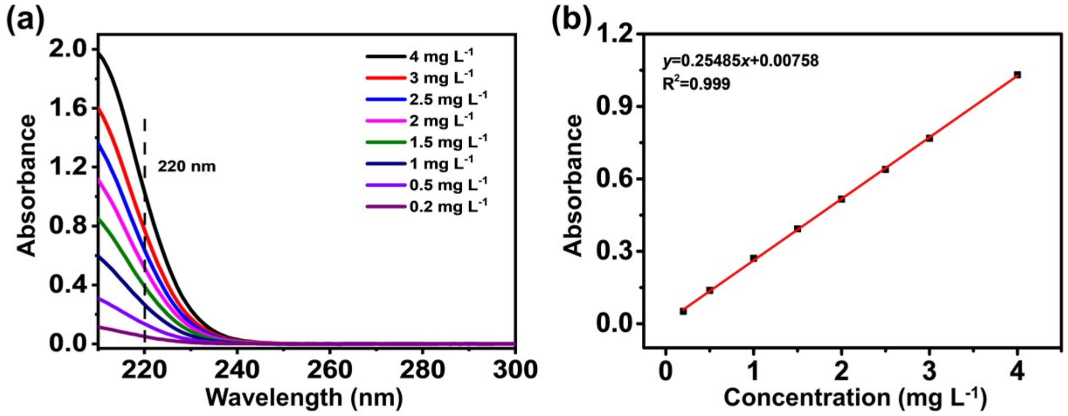

Fig. S4 (a) UV−vis absorption spectroscopy for various concentrations of NO_3^--N. (b) Calibration curve used to estimate the concentrations of NO_3^--N.

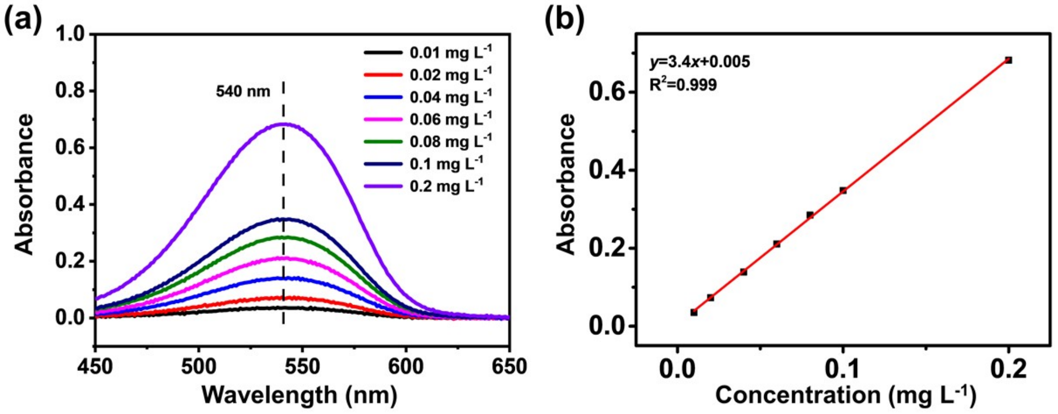

Fig. S5 (a) UV−vis absorption spectroscopy for various concentrations of NO_2^--N. (b) Calibration curve used to estimate the concentrations of NO_2^--N.

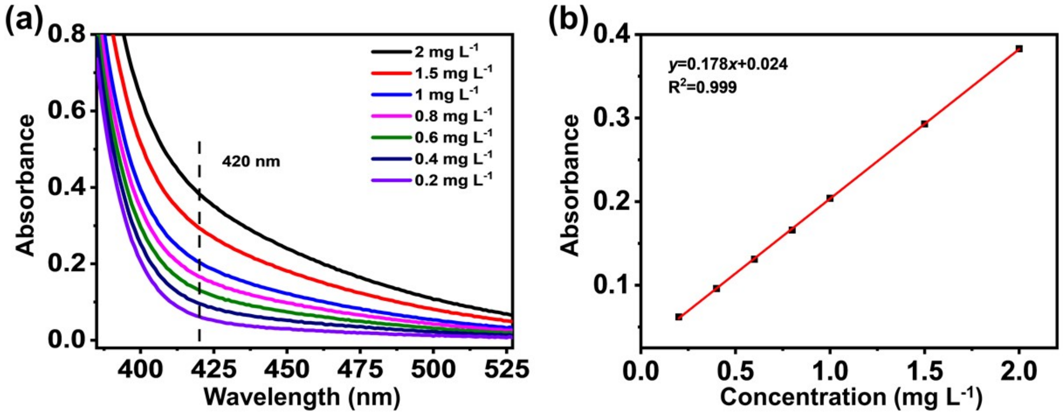

Fig. S6 (a) UV−vis absorption spectroscopy for various concentrations of NH_3-N. (b) Calibration curve used to estimate the concentrations of NH_3-N.

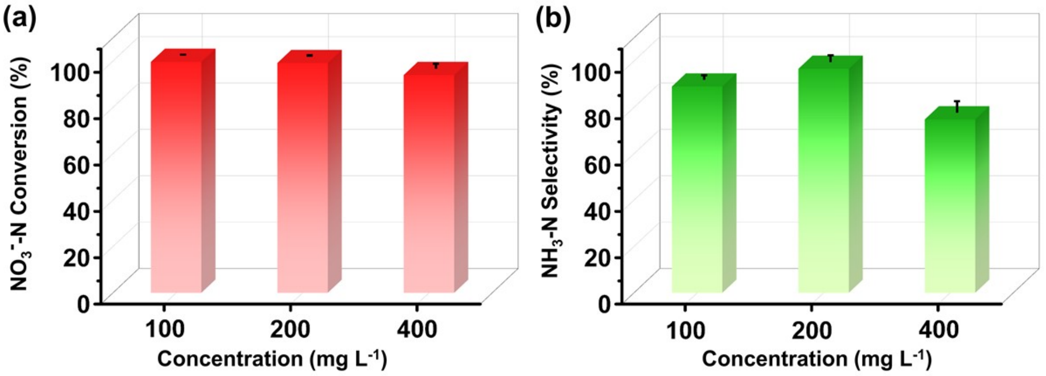

Fig. S7 (a) NO$_3^-$-N conversition and (b) NH$_3$-N selectivity on the CuO@MnO$_2$/CF with various NO$_3^-$-N concentrations.

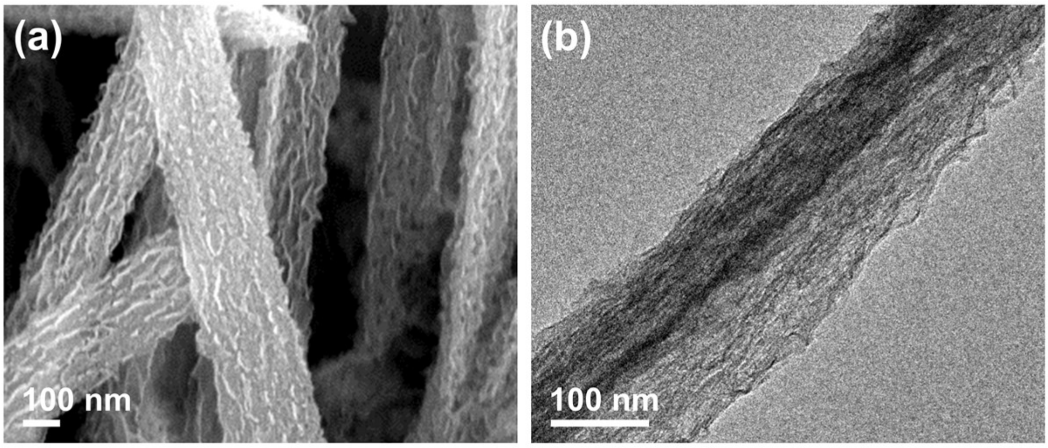

Fig. S8 (a) SEM image of the CuO@MnO$_2$/CF after stability testing. (b) TEM image of the CuO@MnO$_2$ nanowires obtained from CuO@MnO$_2$/CF after stability testing.

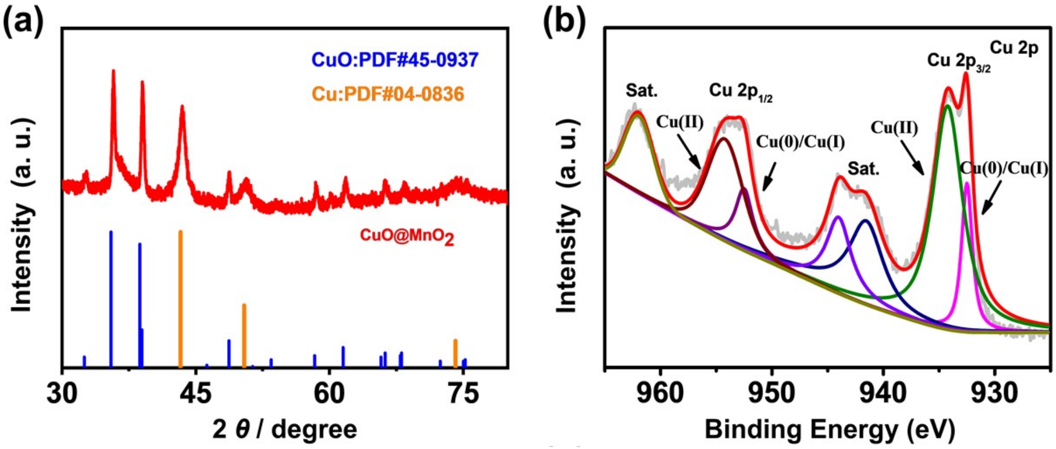

Fig. S9 (a) XRD pattern and (b) Cu 2p XPS spectrum for CuO@MnO$_2$ nanowires after nitrate electroreduction testing.

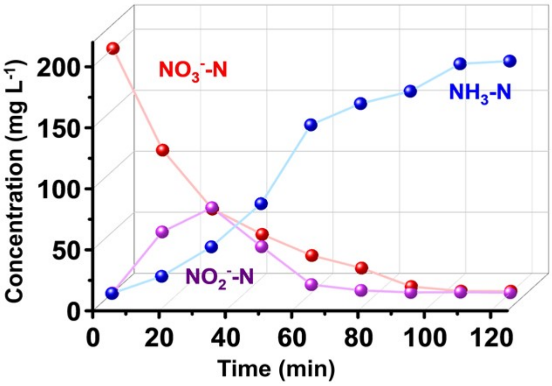

Fig. S10 Time-depended concentrations of NO_3^--N, NO_2^--N and NH_3-N on the CuO@MnO$_2$/CF at -1.3 V (vs. SCE).

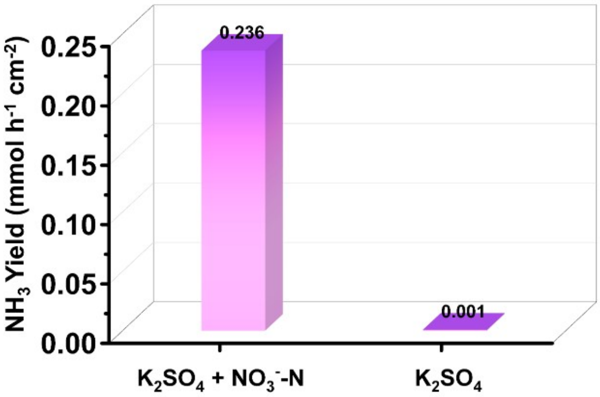

Fig. S11 Ammonia yield rate over the CuO@MnO$_2$/CF in K_2SO_4 electrolyte with and without nitrate.

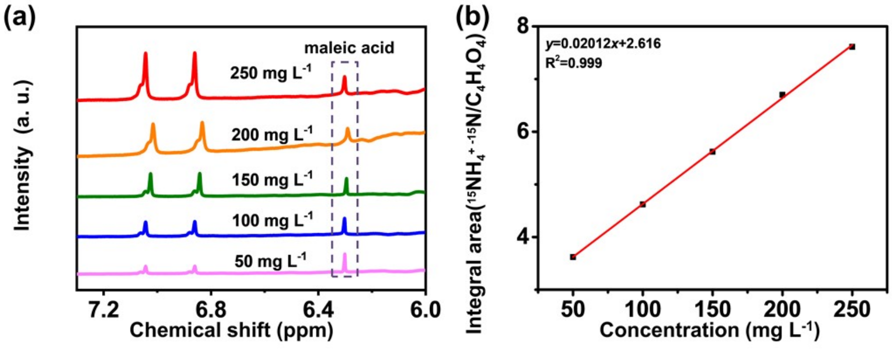

Fig. S12 (a) The ^{1}H NMR spectra of $^{15}NH_4^+$ with different $^{15}NH_4^+$-^{15}N concentration. (b) The standard curve of integral area ($^{15}NH_4^+$-^{15}N / $C_4H_4O_4$) against $^{15}NH_4^+$-^{15}N concentration.

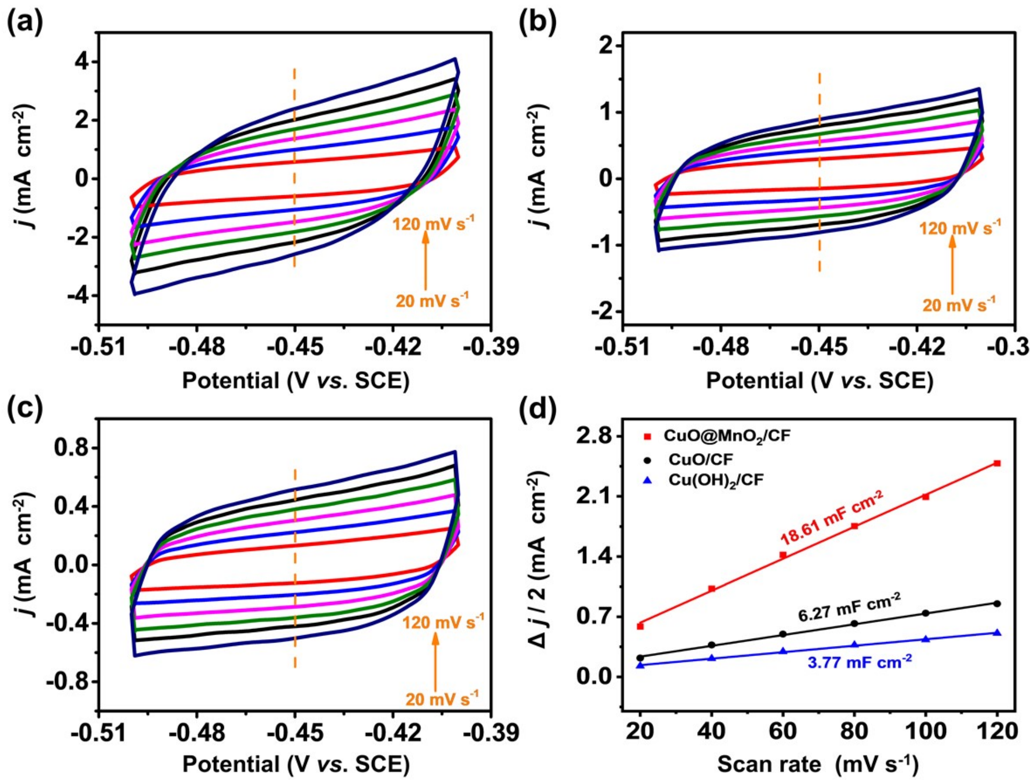

Fig. S13 CV curves at various scan rates for (a) CuO@MnO$_2$/CF, (b) CuO/CF, and (c) Cu(OH)$_2$/CF. (d) Capacitive current densities of the different samples.

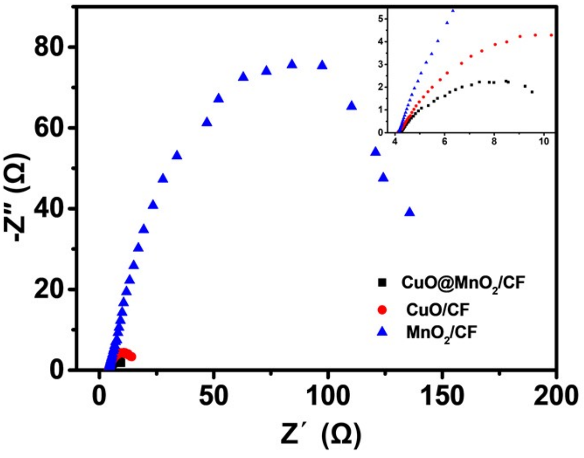

Fig. S14 EIS spectra of the CuO@MnO$_2$/CF, CuO/CF, and MnO$_2$/CF at -1.3 V vs. SCE.

Table S1 The electrochemical nitrate reduction performance comparison between the CuO@MnO$_2$/CF and some other reported electrocatalysts.

Electrocatalysts	**Electrolytes**	**Performance**	**Ref.**
CuO@MnO$_2$/CF	**0.5 M K$_2$SO$_4$, 200 mg L^{-1} NO$_3^-$-N**	**$^{a}r_{NH3}$: 0.240 mmol h^{-1} cm^{-2} $^{b}S_{NH3}$: 96.67 % $^{c}FE_{NH3}$: 94.92 % (-1.3 V *vs.* SCE, 2 h)**	**This work**
Co$_3$O$_4$-TiO$_2$- PVP	0.1 M Na$_2$SO$_4$ 0.1 M NaNO$_3$	S_{NH3}: 73 % (10 mA cm^{-2})	2
TiO$_{2-x}$	0.1 M KOH, 10 mM KNO$_3$	S_{NH3}: 85 % FE_{NH3}: 87.1% (−1.6 V *vs.* SCE, 2 h)	3
Cu/rGO/ graphite plate(GP)	0.02 M NaCl, 0.02 M NaNO$_3$	S_{NH3}: 29.93% (-1.4 V *vs.* SCE, 3 h)	4
Cu–PTCDA	0.1 M PBS, 500 ppm KNO$_3$	r_{NH3}: 436±85 µg h^{-1} cm^{-2} FE_{NH3}: 77 ± 3% (−0.4 V *vs.* RHE, 2 h)	5
Pd-Cu/SS	0.01 M NaClO$_4$, 0.6 mM NaNO$_3$	S_{NH3}: 6% (-0.2 V *vs.* SCE, 3 h)	6
Ir NTs	0.1 M HClO$_4$ 1 M NO$_3^-$-N	FE_{NH3}: 84.7% (-0.06 V *vs.* SCE)	7
Co$_3$O$_4$/Ti	0.05 M Na$_2$SO$_4$, 100 ppm NO$_3^-$-N	S_{NH3}: ~ 70% (10 mA cm^{-2}, 3 h)	8
Cu@Cu$_{2+1}$O NWs	0.5 M K$_2$SO$_4$, 50 mg L-1 NO$_3^-$-N	S_{NH3}: 76% (-1.2 V *vs.* SCE, 2 h)	9
CuPd aerogels	0.5 M K$_2$SO$_4$, 50 µg mL-1 NO$_3^-$-N	S_{NH3}: 76% (−0.46 V *vs.* RHE, 2 h)	10
CuPd@DCLMCS/CNTs	100 mg L-1 NO$_3^-$-N 0.1 M Na$_2$SO$_4$	S_{NH3}: 5% FE_{NH3}: 36% (−1.35 V *vs.* RHE, 24 h)	11
CuO-Co$_3$O$_4$/Ti	100 mg L-1 NO$_3^-$-N, 0.05 M Na$_2$SO$_4$	S_{NH3}:44% FE_{NH3}: 54.5% (20 mA cm^{-2}, 3 h)	12

$^{a}r_{NH3}$: ammonia yield rate; $^{b}S_{NH3:}$ ammonia selectivity; $^{c}FE_{NH3}$: ammonia faradaic efficiency

References

1 Y. Wang, W. Zhou, R. Jia, Y. Yu and B. Zhang, *Angew. Chem. Int. Ed.*, 2020, **59**, 5350-5354.

2 J. N. Gao, B. Jiang, C. C. Ni, Y. F. Qi, Y. Q. Zhang, N. Oturan and M. A. Oturan, *Appl. Catal. B Environ*, 2019, **254**, 391-402.

3 R. R. Jia, Y. T. Wang, C. H. Wang, Y. F. Ling, Y. F. Yu and B. Zhang, *Acs Catal.*, 2020, **10**, 3533-3540.

4 D. Yin, Y. Liu, P. Song, P. Chen, X. Liu, L. Cai and L. Zhang, *Electrochim. Acta*, 2019, **324**, 134846.

5 G.-F. Chen, Y. Yuan, H. Jiang, S.-Y. Ren, L.-X. Ding, L. Ma, T. Wu, J. Lu and H. Wang, *Nat. Energy*, 2020, **5**, 605-613.

6 H. Ji, P. Du, D. Zhao, S. Li, F. Sun, E. C. Duin and W. Liu, *Appl. Catal. B Environ*, 2020, **263**, 118357.

7 J.-Y. Zhu, Q. Xue, Y.-Y. Xue, Y. Ding, F.-M. Li, P. Jin, P. Chen and Y. Chen, *ACS Appl. Mater. Interfaces*, 2020, **12**, 14064-14070.

8 L. Su, K. Li, H. Zhang, M. Fan, D. Ying, T. Sun, Y. Wang and J. Jia, *Water Res.*, 2017, **120**, 1-11.

9 T. Ren, K. Ren, M. Wang, M. Liu, Z. Wang, H. Wang, X. Li, L. Wang and Y. Xu, *Chem. Eng. J.* , 2021, **426**.

10 Y. Xu, K. Ren, T. Ren, M. Wang, M. Liu, Z. Wang, X. Li, L. Wang and H. Wang, *Chem Commun*, 2021, **57**, 7525-7528.

11 H. Xu, J. Wu, W. Luo, Q. Li, W. Zhang and J. Yang, *Small*, 2020, **16**, e2001775.

12 M. Yang, J. Wang, C. Shuang, A. Li, *Chemosphere* **2020**, *255*, 126970